land

MDPI

Article

Application of the Optimal Parameter Geographic Detector Model in the Identification of Influencing Factors of Ecological Quality in Guangzhou, China

Maomao Zhang [1,†] **, Abdulla-Al Kafy** [2] **, Bing Ren** [1] **, Yanwei Zhang** [1] **, Shukui Tan** [1,*] **and Jianxing Li** [3,†]

1   College of Public Administration, Huazhong University of Science and Technology, Wuhan 430079, China
2   Department of Geography & the Environment, The University of Texas at Austin, Austin, TX 78712, USA
3   School of Architecture and Urban Planning, Huazhong University of Science and Technology, Wuhan 430079, China
*   Correspondence: tansk@hust.edu.cn
†   These authors contributed equally to this work.

Abstract: The ecological environment is important for the survival and development of human beings, and objective and accurate monitoring of changes in the ecological environment has received extensive attention. Based on the normalized difference vegetation index (NDVI), wetness (WET), normalized differential build-up and bare soil index (NDBSI), and land surface temperature (LST), the principal component analysis method is used to construct a comprehensive index to evaluate the ecological environment's quality. The R package "Relainpo" is used to estimate the relative importance and contribution rate of NDVI, WET, NDBSI, and LST to the remote sensing ecological index (RSEI). The optimal parameter geographic detector (OPGD) model is used to quantitatively analyze the influencing factors, degree of influence, and interaction of the RSEI. The results show that from 2001 to 2020, the area with a poor grade quality of the RSEI in Guangzhou decreased from 719.2413 km^2 to 660.4146 km^2, while the area with an excellent quality grade of the RSEI increased from 1778.8311 km^2 to 1978.9390 km^2. The NDVI (40%) and WET (35%) contributed significantly to the RSEI, while LST and NDBSI contributed less to the RSEI. The results of single factor analysis revealed that soil type have the greatest impact on the RSEI with a coefficient (Q) of 0.1360, followed by a temperature with a coefficient (Q) of 0.1341. The interaction effect of two factors is greater than that of a single factor on the RSEI, and the interaction effect of different factors on the RSEI is significant, but the degree of influence is not consistent. This research may provide new clues for the stabilization and improvement of ecological environmental quality.

Keywords: ecological quality; remote sensing ecological index (RSEI); influential factors; optimal parameter geographic detector (OPGD)

1. Introduction

As the basic guarantee of human survival and the material basis for the development of society, the ecological environment will directly affect the quality of human life [1,2]. Humans obtain tangible ecosystem products and intangible ecological value services for survival and life from the ecological environment [3]. Therefore, building a stable and safe ecological environment is important for maintaining sustainable social development [4]. In recent decades, with the continuous advancement of urbanization, a large number of people are concentrated in urban areas. However, the disorderly expansion of urban construction land and the massive loss of ecological land has restricted the sustainable development of the overall ecological environment [5–7]. Ensuring the structural stability and functional safety of natural ecosystems to achieve the sustainable development of the ecological environment is a global issue [8,9]. Especially in China's big cities, regional ecological security is faced with the problems of a deteriorating climate environment,

serious soil erosion, and the soaring physical environment of buildings [8,10]. Paying attention to the monitoring and evaluation of the quality of the ecological environment and its dynamic changes has important practical significance for realizing the joint protection and co-governance of the regional ecological environment and sustainable development.

With the development of "3S" technology, many scholars have carried out a series of studies to evaluate the regional ecological status from different angles, combining the advantages of all three [11]. One is single-factor change analysis, such as the analysis of changes in factors closely related to the ecological environment including changes in land use, changes in the net primary productivity of the vegetation, and changes in vegetation coverage [8,9,12–14]. However, for complex ecosystems, especially urban–rural composite ecosystems, the quality of the ecological environment is difficult to measure and quantify using a single ecological index/indicator that only reflects the characteristics of one aspect of the ecosystem [13]. Therefore, another type is the comprehensive analysis of multifactor changes. Compared with single-factor analysis, multifactor comprehensive analysis is more comprehensive and accurate, and scholars have proposed a variety of evaluation index systems for this purpose [15,16]. Xu used a pixel-based model to explore the coupling mechanism between urbanization and the ecological environment of China by applying a combination of mathematics and graphics [17]. Yue analyzed the ecological characteristics of 35 major cities in China and found 18 cities with worsening ecological quality and 17 cities with better ecological quality. From 1990 to 2015, the very poor levels of ecological quality were mainly located in high-density buildings with low vegetation coverage and low soil water content [18]. The primary purpose of Chen's research was to fill the Yue et al. gap through theoretical and empirical research on how urban expansion affects the quality of the ecological environment based on the spatial Durbin model and panel data of 30 provinces in Mainland China from 2003 to 2018 [19]. Sun made a five-level classification of ecological environment quality and then discussed the impact of land use changes on ecological environmental quality [20]. Cao believed that in developing countries, ecological transfer payment (ETP) is the first choice for solving the dilemma of environmental governance [21]. Mukesh et al. compared the RSEI and ecological index (EI) and found that EI may be more effective than RSEI in assessing ecological quality [22]. Wu found that the quality of the ecological environment was significantly affected by multiple indicators, and the impact of any two indicators was greater than a single indicator [23]. In addition, since the advent of the Google Earth Engine (GEE) cloud platform for online geographic computing and analytical processing developed by Google, GEE has been widely used in the fields of large-scale mapping, land use change analysis, and ecological environment monitoring.

The above studies provide the basis for the study of ecological environment quality, but there may also be some shortcomings. Many scholars have proposed a series of methods for monitoring of environmental quality through remote sensing, but these monitoring techniques only focus on a single factor for environmental assessment such as using only the urban heat island index, urban water use and green coverage, and urban impervious surface coverage [20,21]. In the research on the influencing factors, many scholars mainly analyzed using a single explanatory variable, basically conducting research around environmental quality itself, or analyzed the impact of a single variable on environmental quality [22]. Of course, some scholars have established comprehensive indicators to evaluate the RSEI, but there may be obvious deficiencies in the exploration of its influencing factors [23,24]. For example, the interrelationships of factors were not explored and analyzed. In the process of explaining changes in environmental quality, none of the above clearly explains the contribution of environmental quality components to environmental quality [25]. In addition, these studies have not well explained the impact of each variable on the environmental quality and the significance of each variable as well as the magnitude of the impacts.

Given this, this paper took Guangzhou, China, as the research object and used the principal component analysis method to evaluate the changes in the remote sensing eco-

logical index in Guangzhou from 2001 to 2020. The R package "Relaimpo" was used to calculate the contribution of the four constituent indicators to the RSEI. The OPGD model was used to analyze the influencing factors, the degree of influence, and the interaction of explanatory variables for the RSEI. We hope this study can provide new clues for the optimization and improvement of ecological environment quality.

2. Materials and Methods

2.1. Study Area

Guangzhou is located between 112°57′–114°3′ E and 22°26′–23°56′ N (Figure 1). Guangzhou belongs to one of the four major cities in China and has strong economic development strength. The city has 11 districts with a total area of 7434.40 km². Guangzhou has a maritime subtropical monsoon climate with an annual average temperature of 20~22 degrees Celsius. It belongs to a hilly area with an altitude of 1210 m. In recent years, due to the accelerated development of Guangzhou's urbanization process, large areas of woodland and land for planting have been reduced. The urban heat island effect is obvious, as the city's extreme climate performance is more obvious, and extreme climate disasters occur frequently.

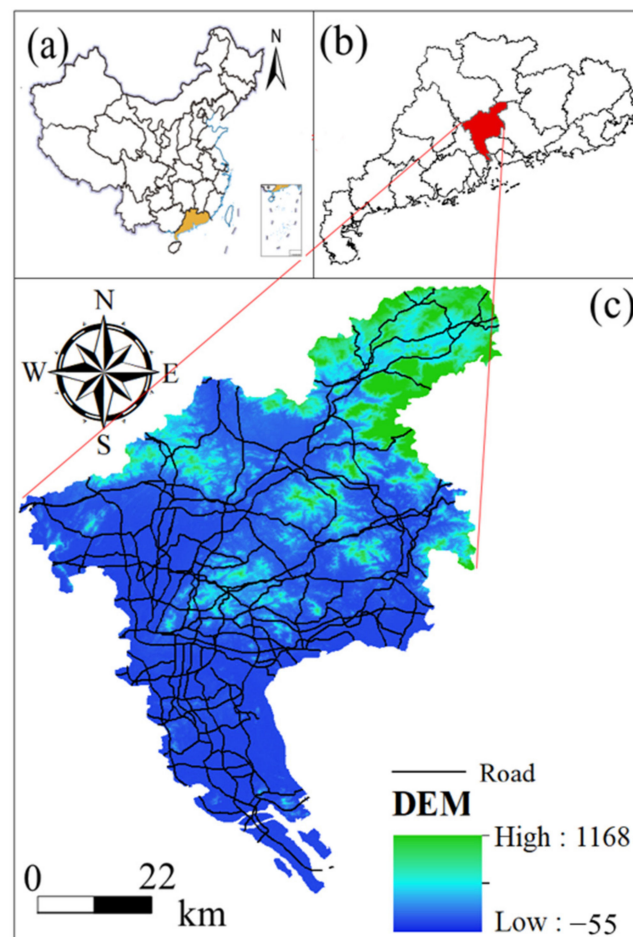**Figure 1.** Location of Guangzhou in China. (**a**). Location of Guangdong Province in China. Note that: the map is based on the standard map with the approval number: GS (2019) No. 1825, downloaded from the Standard Map Service Website of the Ministry of Natural Resources of China, and the base map has not been modified; (**b**) Location of Guangzhou in Guangdong Province; (**c**) Elevation distribution map of Guangzhou.

2.2. Data Sources

Guangzhou was used as the research region in this paper, and two Landsat remote sensing images for 2001 and 2020 were used as the primary data source (https://earthexplorer.usgs.gov/ (accessed on 16 February 2022)). To ensure the comparability of the research, the selected remote sensing data belonged to similar seasons, the natural underlying surface elements were in similar states, the cloud amount was controlled at ≤10%, and the data's accuracy was high (Table 1). We chose the remote sensing data from these periods mainly considering the high quality of the data and the special climate characteristics of Guangzhou. In this paper, the five explanatory variables of the RSEI included precipitation, distance from the road, slope, soil type, and temperature (Figure 2). Elevation data came from the Geospatial Data Cloud (https://www.gscloud.cn/ (accessed on 21 February 2022)), and the road data came from OpenStreetMap (https://www.openstreetmap.org/ (accessed on 18 February 2022)). In ArcGIS v10.2 (ESRI, Redlands, CA, USA), we calculated the distance from the road using the Euclidean distance tool. The precipitation and temperature data came from WorldClim v2.0 (http://www.worldclim.org/ (accessed on 11 February 2022)), and the soil type data came from HWSD v1.2 (http://westdc.westgis.ac.cn/ (accessed on 13 February 2022)). Land type can be found in Appendix A.2, where the d-plot code correlates to the soil type.

Table 1. Remote sensing image data information.

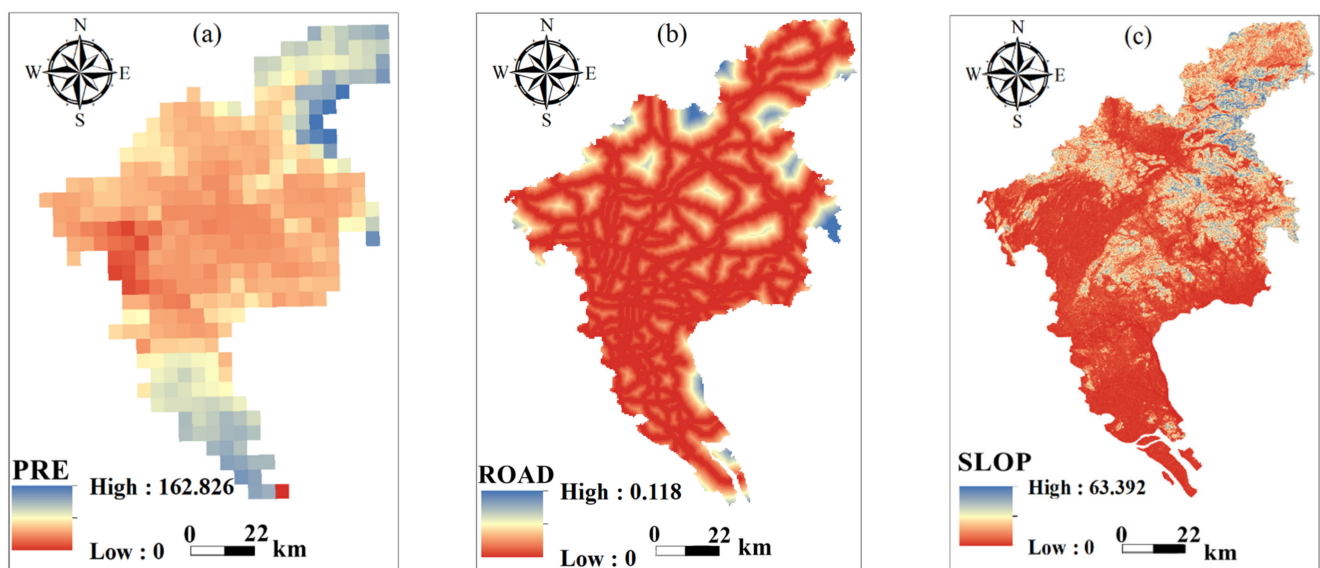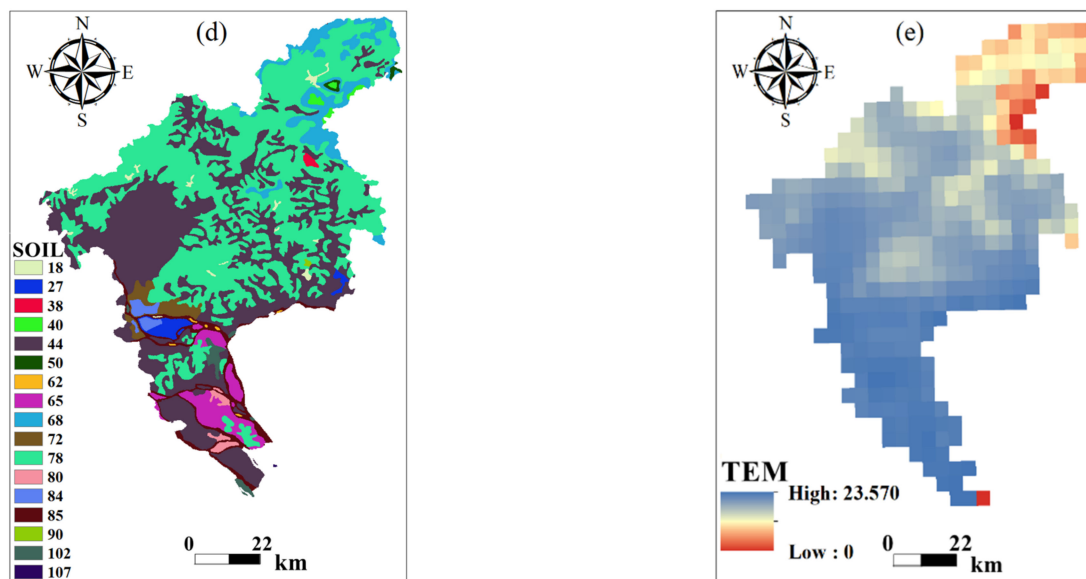| Number	Imaging Data	Satellite/Sensor	Track Number	Cloud Cover (%)
1	30 December 2001	Landsat-5/TM	122-044	≤10
2	28 February 2020	Landsat-8/OLI_TIRS	122-044	≤10

Figure 2. *Cont.*

Figure 2. Distribution of the detection factors. (**a**) Distribution of annual average precipitation; (**b**) Distance distribution from the road; (**c**) Distribution of slope; (**d**) Distribution of soil types; (**e**) Distribution of temperature.

2.3. Research Framework

In this paper, the principal component analysis (CPA) method was used to evaluate the quality of the RSEI. It can objectively determine the weight value to realize the transformation of four single indicators, namely, the NDVI, WET, normalized differential build-up and bare soil index (NDBSI), and land surface temperature (LST), which were coupled to form a comprehensive indicator to objectively evaluate the eco-environmental status in Guangzhou from 2001 to 2020. In addition, this paper used the R package "Relaimpo" to explain the probability of the contribution of various factors of environmental quality, and it can distinguish the relative importance of the relevant regression variables in the multivariate linear model [24]. Finally, we used the optimal parameter geographic detector (OPGD) model to optimize the explanatory variable parameters (i.e., average annual precipitation, distance from the road, slope, soil type, and temperature) to improve the accuracy of the results of the geo-detector model with the optimal spatial discretization parameters and spatial scale parameters. It can effectively extract the geographical features of the explanatory variables and reveal the influencing factors and their changes more comprehensively and objectively. A flow chart of this study is shown in Figure 3.

2.4. Remote Sensing Ecological Index (RSEI)

The remote sensing ecological index (RSEI) selects four important indicators closely related to human survival, including NDVI, WET, NDBSI, and LST, to objectively evaluate the ecological environment [26]. Four index data are usually obtained through remote sensing data: WET through $K - T$ transformation to characterize wetness indicators; NDVI characterizes greenness indicators; NDBSI characterizes the dryness index; LST characterizes the temperature index. In summary, the RSEI can be expressed as a function integrating the above four indicators, namely:

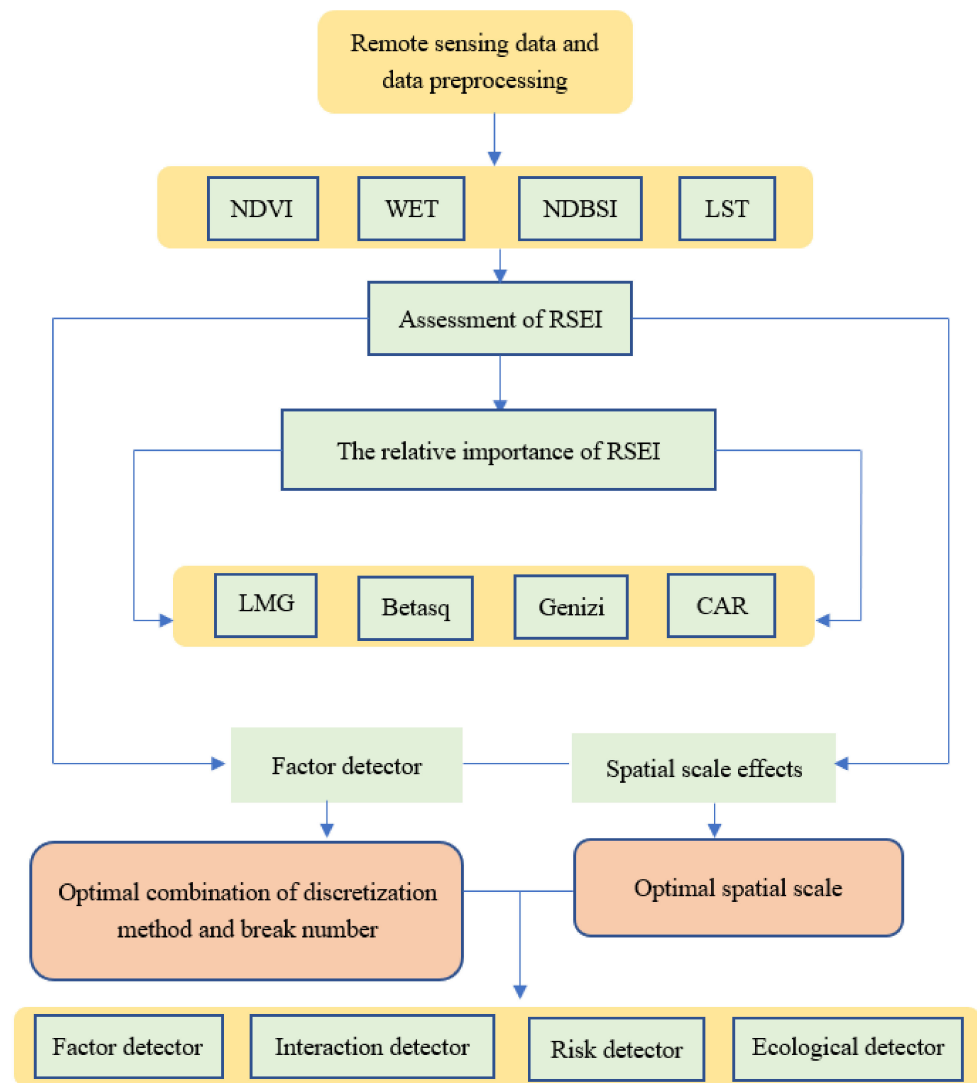$$RSEI = \int (NDVI, WET, NDBSI, LST) \tag{1}$$

Figure 3. A flow chart of this study.

NDVI is a commonly used index to characterize the growth status of vegetation [27]. Therefore, the greenness index can be expressed by the NDVI, the formula is:

$$NDVI = \frac{\rho_{NIR} - \rho_R}{\rho_{NIR} + \rho_R} \tag{2}$$

The wetness index in the ecological environment is closely related to the water content of vegetation and soil; thus, the wetness component can be obtained by $K - T$ transformation [28], and the formula is:

$$WET(Landsat5_{TM}) = 0.0315\rho_B + 0.2021\rho_G + 0.3102\rho_R + 0.1594\rho_{NIR} - 0.6806\rho_{SWIR1} - 0.6109\rho_{SWIR2} \tag{3}$$

$$WET(Landsat8_{OLI}) = 0.1511\rho_B + 0.1973\rho_G + 0.3283\rho_R + 0.3407\rho_{NIR} - 0.7117\rho_{SWIR1} - 0.4559\rho_{SWIR2} \tag{4}$$

where the ρ_B, ρ_G, ρ_R, ρ_{NIR}, ρ_{SWIR1}, and ρ_{SWIR2} represent the first, second, third, fourth, fifth, and sixth bands of the sensor's TM and ETM+ after radiation calibration and the second, third, fourth, fifth, and sixth band of the OLI, 7-band reflectivity.

In the regional environment, buildings and bare soil are important underlying surface factors that cause the ground to dry out. Taking the average of the building index (IBI) and the soil index (SI), the NDBSI represents the dryness index [29], and the formula is:

$$NDBSI = \frac{IBI + SI}{2} \tag{5}$$

$$I = \left[\frac{2\rho_{\text{SWIR1}}}{\rho_{\text{SWIR1}} + \rho_{\text{NIR}}} - \frac{\rho_{\text{NIR}}}{\rho_{\text{NIR}} + \rho_{\text{R}}} - \frac{\rho_{\text{G}}}{\rho_{\text{G}} + \rho_{\text{SWIR1}}} \right] \bigg/ \left[\frac{2\rho_{\text{SWIR1}}}{\rho_{\text{SWIR1}} + \rho_{\text{NIR}}} + \frac{\rho_{\text{NIR}}}{\rho_{\text{NIR}} + \rho_{\text{R}}} + \frac{\rho_{\text{G}}}{\rho_{\text{G}} + \rho_{\text{SWIR1}}} \right] \tag{6}$$

$$\mathbf{SI} = \frac{(\boldsymbol{\rho_{\text{SWIR1}}} + \boldsymbol{\rho_{\text{R}}}) - (\boldsymbol{\rho_{\text{NIR}}} + \boldsymbol{\rho_{\text{B}}})}{(\boldsymbol{\rho_{\text{SWIR1}}} + \boldsymbol{\rho_{\text{R}}}) + (\boldsymbol{\rho_{\text{NIR}}} + \boldsymbol{\rho_{\text{B}}})} \tag{7}$$

The surface temperature that characterizes the heat index can be obtained by correcting the brightness temperature [30]. After radiometric calibration, the radiance $L\lambda$ can be converted to the brightness temperature, T, according to the calibration parameters, k_1 and k_2, the formula is:

$$T = \frac{k_2}{ln\left(\frac{K1}{k_{\frac{6}{10}}} + 1 \right)} \tag{8}$$

The brightness temperature, T, must be corrected by a specific emissivity to be converted to the surface temperature [31], the formula is:

$$LST = \frac{T}{1 + \frac{\lambda T}{\rho}\ln \varepsilon} \tag{9}$$

where $\lambda = 11.5$ μm; $\rho = 1.428 \times 10 - 2$ m·k; ε is the surface emissivity.

In this study, principal component analysis (PCA) was used to evaluate the remote sensing ecological indicators in Guangzhou. Based on the characteristics of the original data of the four indicators (i.e., NDVI, WET, NDBSI, LST), the weight value was determined automatically and objectively to realize the transformation of multiple single indicators coupled into a comprehensive indicator, which avoided subjective arbitrariness, and the process was relatively simple [32–34]. Before conducting the principal component transformation, range standardization was performed on the four indicators first to avoid the imbalance of the indicator weights. We performed PCA transformation on new images by data fusion and to compute PC1. To make the ecological environment quality proportional to the value, it was necessary to further transform in order to obtain the initial ecological index $RSEI_0$. The formula is as follows.

$$RSEI_0 = 1 - \left\{ PC1 \left[\int (NDVI, WET, NDBSI, LST) \right] \right\} \tag{10}$$

Finally, it was necessary to standardize the range of $RSEI_0$ to obtain the remote sensing ecological index (RSEI), which has a value range of [0, 1]. The formula is as follows.

$$RSEI = \frac{RSEI_0 - RSEI_{min}}{RSEI_{max} - RSEI_{min}} \tag{11}$$

In the formula, the closer the RSEI value is to 1, the better the quality of the ecological environment, and vice versa, the worse the quality of the ecological environment.

2.5. Analysis of the Relative Importance of the RSEI

The R package "Relaimpo" was used to estimate the relative importance of the NDVI, WET, NDBSI, and LST to the RSEI. The "relative importance" in the multiple regression model refers to the quantification of the contribution of a single regression variable to the overall multiple regression model [35–37]. Generally, as long as all regression variables were uncorrelated, there is no problem with the evaluation of relative importance in a linear model; the contribution of each variable was the R^2 of a single regression, and all the individual R^2 values add up to the entire model's R^2. However, the contribution of the RSEI's influence degree will be affected by the influence of the climatic environment in different time bands, which may lead to correlation. However, the "LMG", "Betasq", "Genizi", and "CAR" methods in "Relaimpo" can distinguish the relative importance of related regression variables in a multivariate linear model. The calculation process of this method is relatively complicated, but it can better distinguish the relative importance of

related variables and has been widely used [37–39]. The specific process of this method is as follows:

$$SeqR^2((M\backslash S)) = R^2(M \cup S) - R^2(S) \tag{12}$$

$$SeqR^2\left(\left\{x_k\right\}\backslash S_k(r)\right) = R^2(\{x_k\} \cup S_k(r)) - R^2(S_k(r)) \tag{13}$$

$$LMG(x_k) = \frac{1}{P}\sum_{j=0}^{P-1}\left(\sum_{\substack{S \subseteq \{X_1,\dots,X_p\}\backslash\{X_k\} \\ n(S)=j}} \frac{seqR^2(\{X_k\}\backslash S)}{\binom{p-1}{i}}\right) \tag{14}$$

where $SeqR^2((M\backslash S))$ is the regressor in the additional R^2 set S when the regressor in set M is added to the model, and $seqR^2(\{x_k\}\backslash S_k(r))$ is allocated in order. $LMG\ (x_k)$ given to the regressor x_k represents the contribution of the variables to the multiple linear regression model [35,36].

$$\hat{\beta}_{k,standardized} = \hat{\beta}_k\frac{\sqrt{S_{kk}}}{\sqrt{S_{yy}}} \tag{15}$$

In the formula, S_{kk} and S_{yy}, respectively, represent the empirical variance of the regression equation X_k and the response $\boldsymbol{y}$. As long as one only compares the regressions within models for the same response y, the division is by $\sqrt{S_{yy}}$. The square of the standardized coefficient is recommended as a measure of relative importance [40,41].

Genizi proposed a variable importance measure [42], and the formula is as follows.

$$\varnothing^G\left(X_j\right) = \sum_{k=1}^d\left((p^{\frac{1}{2}})_{jk}(p^{-\frac{1}{2}}p_{XY})_k\right)^2 \tag{16}$$

where $p^{\frac{1}{2}}$ is the symmetric and positive definite with the square root of the matrix uniquely defined by $p^{\frac{1}{2}}$. Genizi's metric provides a decomposition, which is converted to $\sum_{j=1}^d\varnothing^G\left(X_j\right) = \Omega^2$ and then converted to the square edge correlation in the case of uncorrelation, and it obeys orthogonality guidelines. Contrary to $\varnothing^{HP}\left(X_j\right)$, the "Genizi" measure is also nonnegative by construction, $\varnothing^G\left(X_j\right) \geq 0$ [43].

$$Y_{std}^* = \omega^T\delta(X) = \sum_{j=1}^d\omega_j\delta_j(X) \tag{17}$$

$$\delta(X) = p^{-\frac{1}{2}}V^{-\frac{1}{2}}(X - \mu) = p^{-\frac{1}{2}}X_{std} \tag{18}$$

The Markov correlation, standardized predictor, and $Var(\delta(X)) = I$; therefore, the CAR score, ω, is the weight that describes the influence of each decorrelation variable in predicting the standardized response [40]. In addition, for $Corr(X_{std}, Y) = P_{XY}$, the CAR score was the correlation between the response and decorrelation covariates.

$$\omega = Corr(\delta(X), Y) \tag{19}$$

2.6. Optimal Parameter Geographic Detector (OPGD)

The OPGD model includes five parts: factor detector, parameter optimization, interaction detector, risk detector, and ecological detector. The parameter optimization included two parts: spatial discretization optimization and spatial scale optimization [25,28,44].

2.6.1. Factor Detector

As the core part of geographic detector, the factor detector revealed the relative importance of the explanatory variables through Q statistics [45–47]. The Q statistic compares the dispersion variance between the observed value of the entire study area and the variable level, and the Q value of each explanatory variable is calculated as follows:

$$Q_x = 1 - \frac{\sum_{j=1}^M N_{x,j}\sigma_{x,j}^2}{N_x\sigma_x^2} \tag{20}$$

where Q_x and σ_x^2 are the number and variance of observations in the entire study area, and $N_{x,j}$ and $\sigma_{x,j}^2$ are the number and variance of the internal observations ($j = 1, 2, \ldots, m$) of the subregion of variable x. A larger Q value means that there was a stronger explanatory power, because the difference in the subregions was small. In a geographic detector, at least two samples are required for each formation in order to calculate the average and variance.

The F test was used to determine whether the changes between the observed value and the stratified observation value were significantly different, because the transformed Q value can be tested with a noncentral F distribution [48].

$$F = \frac{N-M}{M-1}\frac{Q}{1-Q} \sim F(M-1, N-M; \delta) \tag{21}$$

where M is the number of subregions, N is the number of observations, and δ is the noncentral parameter [49].

$$\delta = \frac{\left[\sum_{j=1}^M \overline{Y}_j^2 - \frac{1}{N}\left(\sum_{j=1}^M \overline{Y}_j \sqrt{N_j}\right)^2\right]}{\sigma^2} \tag{22}$$

where $\overline{Y}_j$ is the average value of observations in the j_{th} subregion of the variable. Therefore, given the significance level, the null hypothesis, $H_0 : \sigma_x^2 = \sigma_{x,j}^2$, can be checked by the following formula, $F(M-1, N-M; \delta)$, in the distribution table [50].

2.6.2. Parameter Optimization

Parameter optimization included spatial discretization optimization and spatial scale optimization. In this study, the OPGD model chose the best combination of the discretization method and the number of interruptions of each geographic variable as the optimal discretization parameter [25,51]. The Q value calculated by the factor detector was used to determine the best parameter combination. It provided a set of decomposition methods and a combination of the number of interrupts for each continuous variable to calculate the respective Q value [52].

2.6.3. Interaction Detector

The interaction detector determines the interaction influence of two overlapping space explanatory variables based on the relative importance of the interaction calculated with the Q value of the factor detector. Spatial interaction is the superposition of two spatial explanatory variables. The interaction detector explores the influence of the interaction condition on the dependent variable through the comparison between the Q value of the interaction and the two univariates [53,54].

2.6.4. Risk Detector

The risk detector was used to test whether the spatial pattern represented by the average value was classified as a subarea of categorical or hierarchical variables. The difference between the average values of subregions η and k was tested by the t-test [55].

$$t_{\overline{Y}_\eta - \overline{Y}_k} = \frac{\overline{Y}_\eta - \overline{Y}_k}{\sqrt{\frac{S_\eta^2}{N_\eta} + \frac{S_k^2}{N_k}}} \tag{23}$$

where $\overline{Y}_\eta$ and $\overline{Y}_k$ are the average values of the observations of the subregions η and k; S_η^2 and S_k^2 are the variances; N_η and N_k are the number of observations [56].

2.6.5. Ecological Detector

The ecological detector was used to test whether one explanatory variable had a greater impact than another variable. The significance of the different effects of the explanatory variables was tested with the F statistic [57].

$$F = \frac{N_x(N_y - 1)\sum_{j=1}^{M_x} N_{x,j}\sigma_{x,j}^2}{N_y(N_x - 1)\sum_{j=1}^{M_y} N_{y,j}\sigma_{y,j}^2} \qquad (24)$$

where N_x and N_y are the number of observations; M_x and M_y are the number of subregions; $\sum_{j=1}^{M_x} N_{x,j}\sigma_{x,j}^2$ and $\sum_{j=1}^{M_y} N_{y,j}\sigma_{y,j}^2$ are the sum of variances in the subregions of variables x and y [58].

3. Results

3.1. Principal Component Analysis of Ecological Indicators

Through PCA analysis, the ecological environment quality of the four indicators in the study area was analyzed, and the contribution rate of the eigenvalues of the first principal component (PC1) was much larger than that of the eigenvalues of the other three principal components (Table 2). The proportion of the eigenvalues of the first principal component in the two years was more than 80%, which indicates that the first principal component analysis method had a significant effect and was representative of the calculation of the remote sensing ecological index. The values of the other principal components fluctuated, indicating that the information on the four ecological indicators was incomplete. Table 2 reveals that both the NDVI and WET in PC1 were positive, which indicates that the NDVI and WET had a positive effect on the ecological environment. The LST and NDBSI indices were both negative, indicating that LST and NDBSI had negative impacts on the ecological environment.

Table 2. Principal component analysis results of indicators.

Year	Indicator	PC1	PC2	PC3	PC4
	NDVI	0.6488	0.1954	0.4313	0.5957
	WET	0.3282	0.7035	0.4436	0.4478
	NDBSI	−0.6070	−0.4453	−0.3223	−0.5739
2001	LST	−0.3208	−0.5182	−0.7165	−0.3395
	Eigenvalue	0.8197	0.2769	0.1995	0.0974
	Percent (%)	81.2400	10.7300	6.1500	1.8700
	NDVI	0.4837	0.2436	0.5166	0.7065
	WET	0.8748	0.1567	0.2606	0.4083
2020	NDBSI	−0.0268	−0.4362	−0.8156	−0.5780
	LST	−0.2475	−0.5321	−0.2375	−0.3741
	Percent (%)	82.5500	13.3600	3.1700	0.9300
	Eigenvalue	0.6954	0.3596	0.0417	0.0014

3.2. Temporal and Spatial Changes in Ecological Environment Quality

Referring to related studies [18,59], we divided Guangzhou's RSEI into four grades (i.e., 0~0.25—bad; 0.25~0.50—good; 0.50~0.75—very good; 0.75~1.00—excellent). The spatial distribution of the graded remote sensing ecological indices is shown in Figure 4. Figure 4 reveals that the overall quality of the ecological environment in Guangzhou has improved from 2001 to 2020, and the area of bad ecological environment quality level has decreased. This area was mainly distributed in the southern part of Guangzhou. The area of good grade and excellent grade ecological environment quality level increased significantly, and this area was mainly distributed in the northern part of Guangzhou. The terrain in the southwest and south of Guangzhou is low and flat, most of which are plain terrain areas, and this area is an area with fast economic development in Guangzhou. The urbanization process in these areas is faster, the urban building density is high, the road traffic density is high, and the population is relatively dense; thus, the ecological level is relatively low. The northern part of Guangzhou has higher terrain, is mostly mountainous terrain, has high vegetation coverage, low urban building density, and relatively high ecological environment quality.
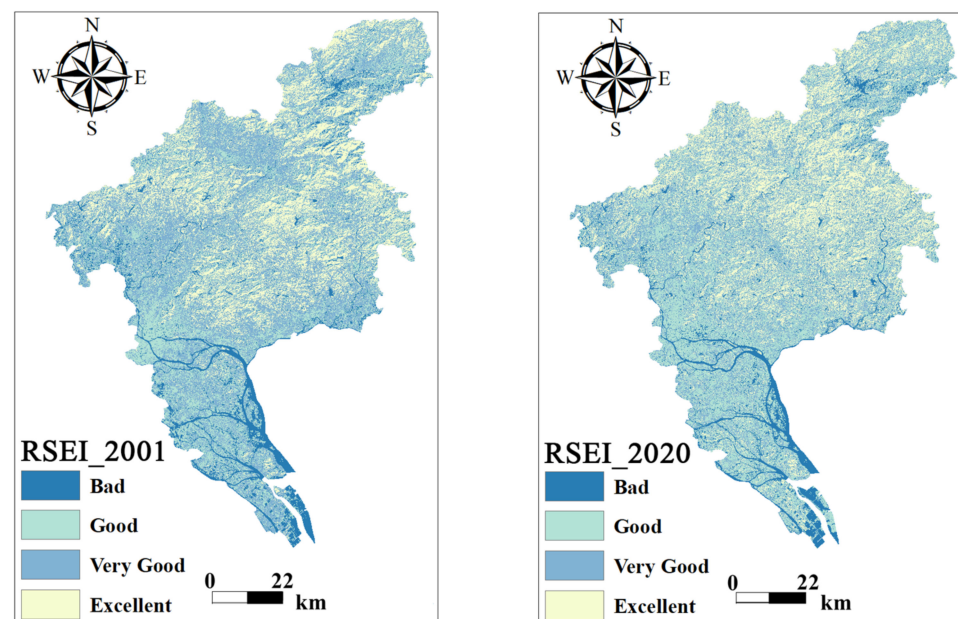
Figure 4. Distribution map of the ecological environmental quality from 2001 to 2020.

In ArcGIS v10.2, the changes in the area and proportion of different ecological environment quality levels in Guangzhou from 2001 to 2020 were calculated (Table 3). Table 3 reveals that the area with a bad ecological environment quality level decreased from 719.2413 km^2 in 2001 to 660.4146 km^2 in 2020, with an area reduction of 58.8267 km^2, and the proportion of the decline was 0.81%. The area with a good ecological environment quality level increased from 1762.1784 km^2 to 2247.3468 km^2, an increase of 6.72%. The area with a very good ecological environment grade decreased from 2961.3069 km^2 in 2001 to 2334.8574 km^2, a year-on-year decrease of 8.68%. The area with an excellent ecological quality level increased from 1778.8311 km^2 in 2001 to 1978.9389 km^2 in 2020, an increase of 200.1087 km^2.

Table 3. Area and proportion of different grades of ecological environment quality.

Quality Level	2001		2020	
	Area (km^2)	Proportion (%)	Area (km^2)	Proportion (%)
Bad	719.2413	9.9600	660.4146	9.1500
Good	1762.1784	24.4000	2247.3468	31.1200
Very Good	2961.3069	41.0100	2334.8574	32.3300
Excellent	1778.8311	24.6300	1978.9389	27.4000

3.3. Analysis of the Relative Importance of the RSEI

Based on the relative importance analysis models of LMG, Betasq, Genizi, and CAR in the "Relainpo" package in the R software, this paper analyzed the contribution rate of the remote sensing ecological index indicators to the ecological index in 2001 and 2020 respectively (Figure 5). Figure 5 shows that the results of the four relative importance models in 2001 and 2020 all showed that the NDVI had the largest contribution to the ESRI in Guangzhou, while the NDBSI had the smallest contribution to the ESRI. This means that the NDVI does have an important effect on the RSEI, while the NDBSI has a weaker effect on it.

Figure 5a shows that the four ecological indicators in 2001 had different degrees of contribution to the RSEI in Guangzhou. In 2001, the ecological indicator with the largest contribution to the RSEI was NDVI. The results of the four models of LMG, Genizi, Betasq, and CAR showed that the contribution rates of NDVI to the RSEI were 49.35%, 50.08%, 50.14%, and 50.57%, respectively. Secondly, the influencing factor that has a greater impact

on the RSEI was WET. The results of the four models of LMG, Genizi, Betasq, and CAR show that the contribution rates of WET to the RSEI were 32.54%, 21.06%, 31.04%, and 32.76%, respectively. The impact of LST on the RSEI was relatively small, and its contribution rate was approximately 15%. In addition, the results of the four models all showed that the NDBSI had a weak effect on the RSEI, and its contribution rate was less than 5%.
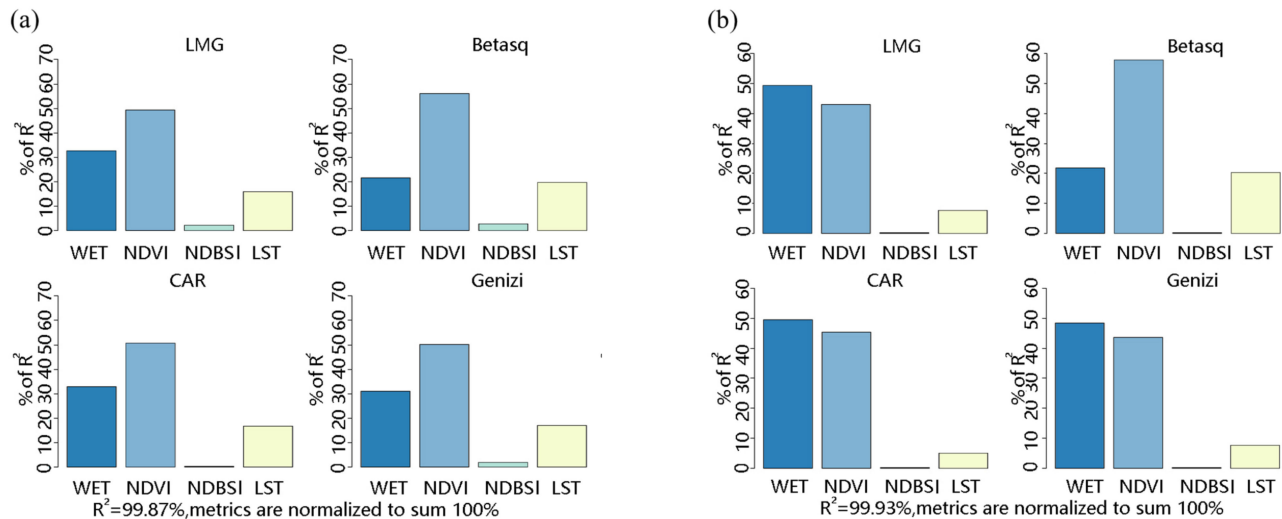

Figure 5. The relative importance of the RSEI. (**a**) Results of relative importance in 2001; (**b**) Results of relative importance in 2020.

Figure 5b shows the distribution of the impact of the four ecological indicators on the RSEI in 2020. Compared with 2001, the contribution rate of WET to the RSEI increased significantly. Specifically, except for the contribution rate shown by the Betasq model which dropped by 3.07% compared with 2001, the other three models all showed that its contribution rate increased by approximately 20%, indicating that WET had a stronger impact on the RSEI in 2020. The contribution of LST to the RSEI increased in the Betasq model, and the other three models all showed a decrease of approximately 5%. This generally reflects that the contribution rate of LST to the RSEI was small and had a slight downward trend, but we cannot ignore its influence. Compared with the contribution rate of NDBSI to the RSEI in 2001, it was still the smallest ecological indicator, and the four models all showed that the contribution rate of the NDBSI to the RSEI was less than 4%. This shows that the impact of the NDSBI on the RSEI in Guangzhou was relatively stable, and the contribution rate fluctuated little.

3.4. Analysis of the OPGD

First, we used the OPGD model to analyze the spatial explanatory variables of the remote sensing ecological index. The OPGD model needs to use optimal parameterization to discretize these five explanatory variables [25]. The discretized results are shown in Figure 6. We utilized the optimal parameterization to effectively turn the five explanatory variables into stratigraphic variables, which were equivalent to categorical variables in geographic detectors.

Figure 7 shows the comparison of the effects of each variable of the RSEI at different spatial unit scales. Figure 7 reveals that the values of the five variables, including annual average precipitation, temperature, slope, road, and soil, increased from 5 to 20 km space units, showing a clear upward trend. In addition, the 90% quantile value reached a maximum value when the space unit reached 20 km, while beyond the 20 km space unit there is a decreasing characteristic. Therefore, in this study, we use 20 km as the scale unit for spatial stratified heterogeneity analysis.
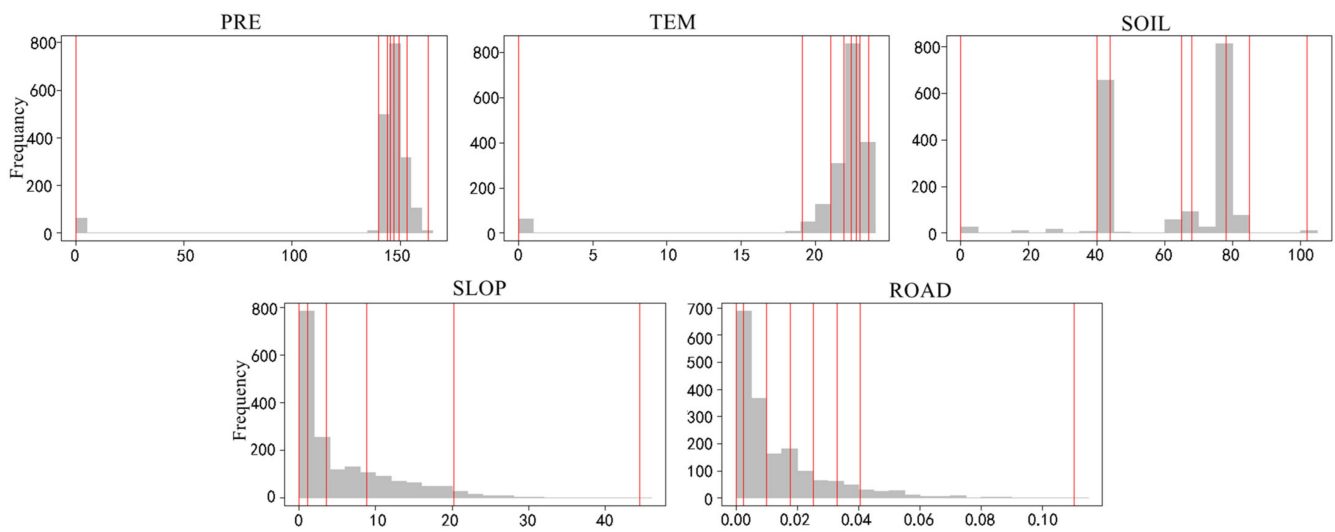
Figure 6. Optimization results of spatial data discretization parameters.
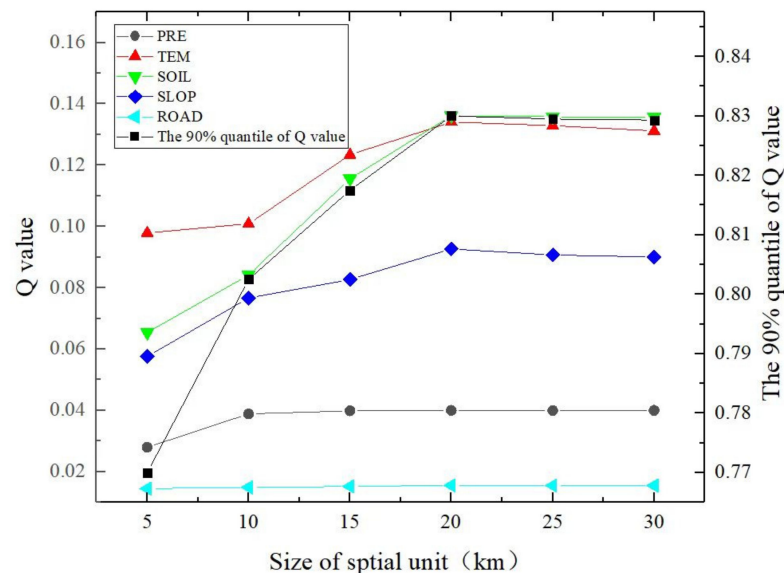

Figure 7. Comparison of the scale effects for spatial units and 90% quantiles of the explanatory variables.

Second, we used factor detectors to analyze the impact of individual explanatory variables on the remote sensing ecological index. The results show that the maximum Q value of the soil type on the remote sensing ecological index image was 0.1360, followed by a precipitation Q value of 0.1341, and the road Q value with the least impact was 0.0155 (Figure 8).

Third, we used a risk detector to determine the means of risk for variables within the space and to test whether the means of risk differ significantly for various regions of the space (Figure 9). Figure 9a shows that the annual average precipitation had the greatest impact on the RSEI when the average annual precipitation was 146~147 mm. When the annual average temperature was between 21.0 and 21.9 °C, the effect of temperature on the RSEI was most obvious. Soil types had obvious positive effects on the RSEI, and soil types 68~78 had a significant effect on the RSEI. However, when the soil types were 78~85, it had a significant negative impact on the RSEI. The impacts of slope on the RSEI were all positive stimuli, and when the slope was between 8.88° and 20.20°, it had the greatest impact on the RSEI. The positive effect of the slope on the RSEI was weakest when the slope was between 0° and 1.50°. Next, this paper analyzed the impacts of distance from the road on the RSEI.

Figure 9a shows that when the distance from the road was between 0.0176 and 0.0253, the road had the most significant impact on the RSEI, while it had the least impact on the RSEI when it was between 0.0253 and 0.0329. Figure 9b reflects whether a single factor had an impact on the RSEI in this interval. In the figure, N means no impacts, and Y means it had impacts on the RSEI. Taking the precipitation factor as an example, Figure 9b reveals that when the precipitation was in the two ranges of 0~140 mm and 153~163 mm, the effect of precipitation on the RSEI was extremely weak. However, when the precipitation was in the two ranges of 140~144 mm and 153~163 mm, the precipitation had a significant impact on the RSEI.
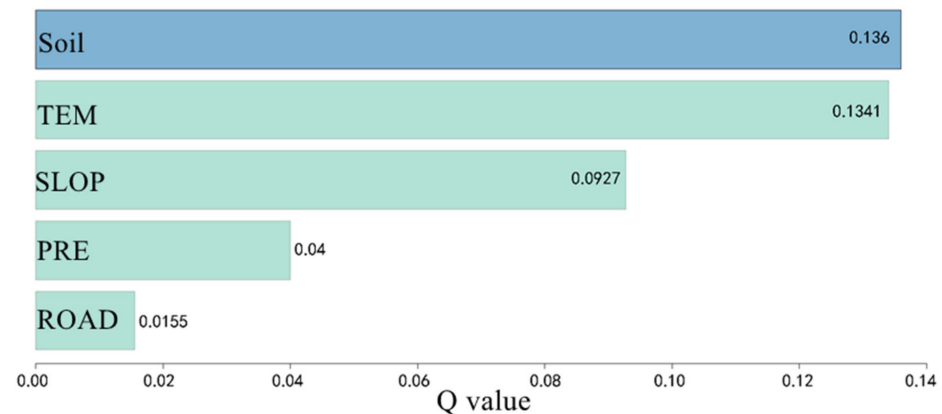

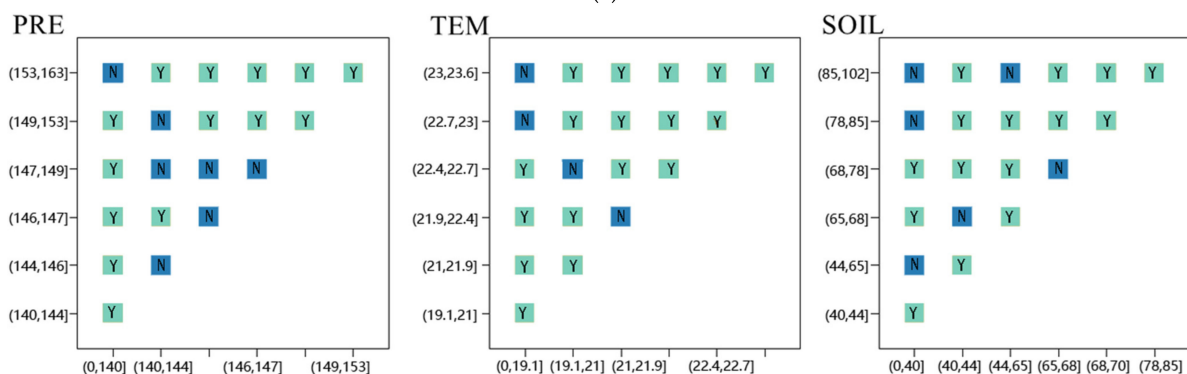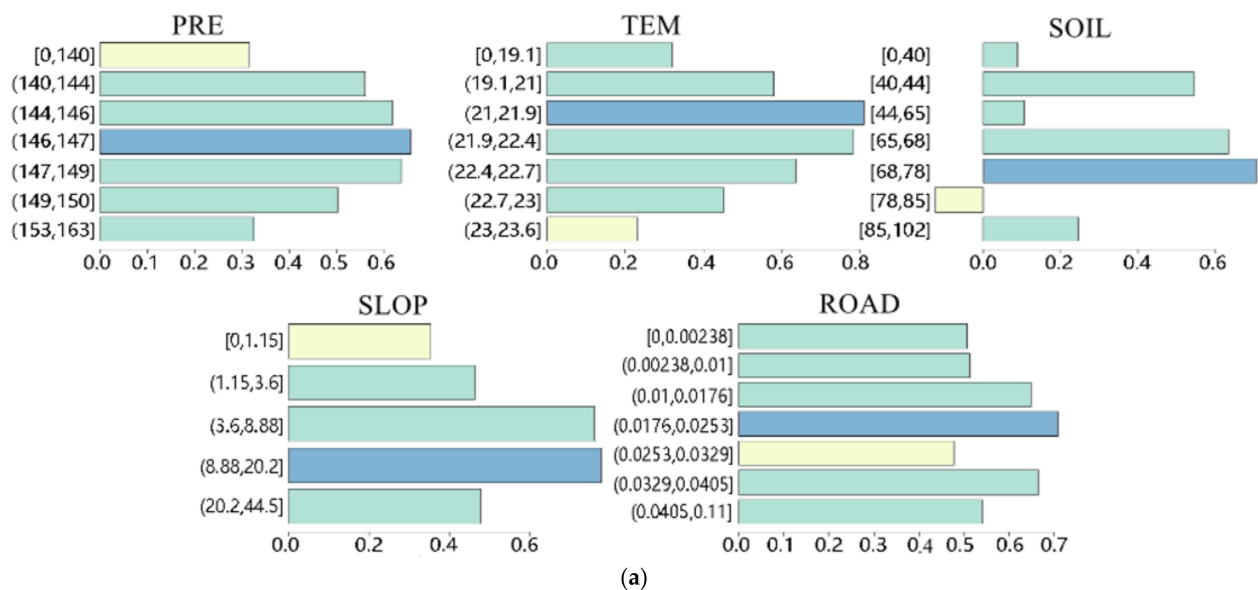**Figure 8.** The impact of a single factor on the RSEI.

(a)

Figure 9. *Cont.*

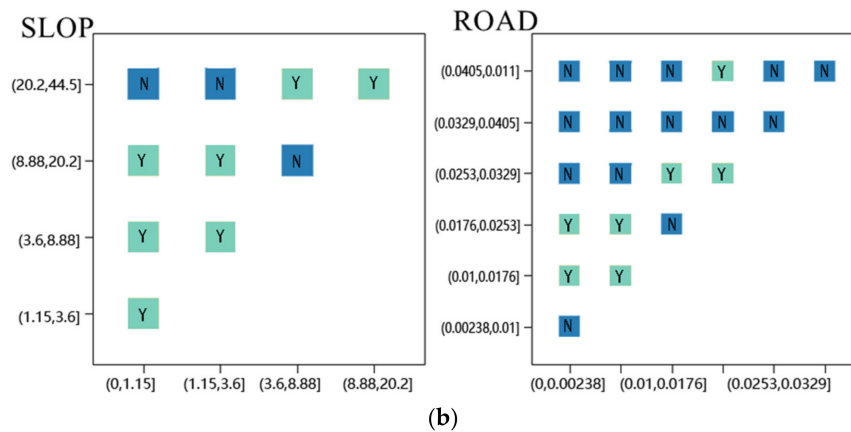**Figure 9.** (**a**) Mean value of the RSEI; (**b**) risk detector results.

Fourth, the article performed interactive detection of the influencing factors, and the specific results are shown in Figure 10a. It reveals that the interaction between soil type and the annual mean temperature had the most obvious effect on the RSEI, and the Q value of their interaction effect was 0.1903. The second largest interaction effect on the RSEI was soil type and average annual precipitation, and the Q value of their interaction effect was 0.1789. The two factors, road and annual mean precipitation, had the smallest interaction effects on the RSEI, with Q values of 0.0828.
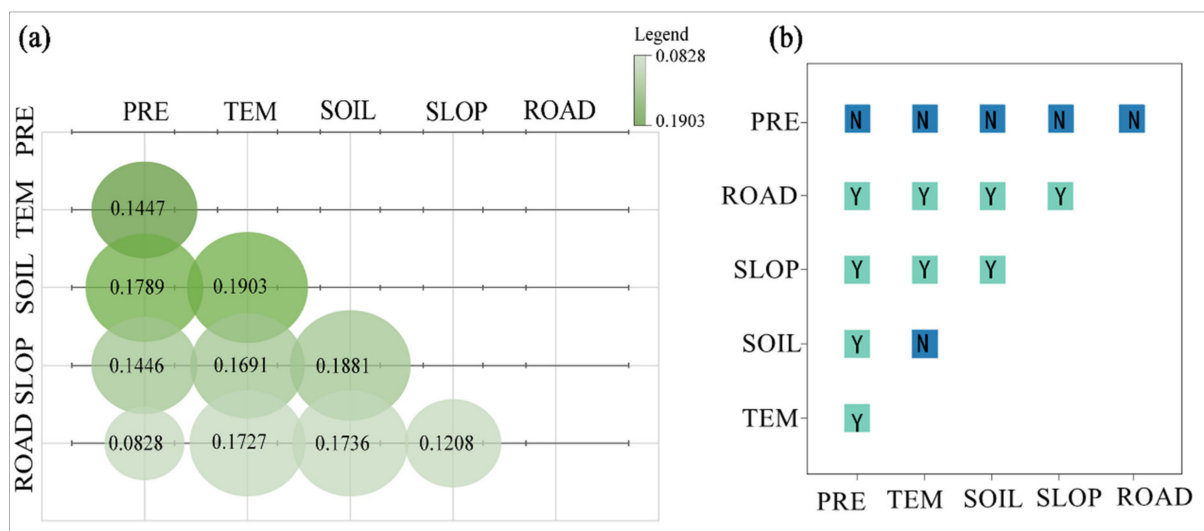

Figure 10. (**a**) Results of interaction probe; (**b**) results of the ecological probe.

Finally, the analysis of the ecological detector was carried out, and the specific results are shown in Figure 10b. The figure shows that the combination of the annual mean precipitation variable and the other four variables does not produce a situation where precipitation has a greater impact on the RSEI than any other variable. Soil type and annual mean temperature do not show that one variable has more significant impacts on the RSEI than the other. In addition, any two variables in other variables have different degrees of influence on the RSEI.

4. Discussions

In this study, we quantify the RSEI of Guangzhou in 2001 and 2020 by principal component analysis, and the results are divided into four grades. The area with a bad grade for ecological environment decreased, and the areas with a very good and excellent grade of ecological environment increased significantly, perhaps because of the influence

of environmental protection policies [60]. In addition, the concept of "lucid waters and lush mountains are invaluable assets" was first proposed in 2005. The Chinese government proposed to establish and practice the concept of "lucid waters and lush mountains are invaluable assets", adhere to the basic national policy of saving resources and protecting the environment, and resolutely prohibit a series of human activities that damage the natural environment. In future urban planning, we need to continue to strengthen urban environmental governance and pay attention to the inhibitory effect of vegetation coverage on the destruction of the ecological environment in urban development [61].

Based on the analysis of the R package "Relaimpo", the results show that the contribution rate of the NDVI and WET to the RSEI increased year by year, and the area of green space in Guangzhou increased during the research period. According to statistics in 2020, the total area of green land was 147,048 km^2, and the area of park green land was 30,189 km^2. On the other hand, we also found that the contribution rate of LST to the RSEI was also increasing. This may be due to the high population density in the southwest area of Guangzhou and the continuous expansion of the urban impervious construction area [62]. This urban physical environment exacerbates the urban heat island effect, and it also stimulates the effect of LST on the RSEI to a certain extent [63]. Therefore, we should attach importance to the addition of urban green belts, build urban green spaces, and moderately control the expansion of construction land to reduce the negative impact of LST on the RSEI.

The OPGD model reveals the geographic features and information among these variables by optimizing the parameters of five single-factor explanatory variables and optimizing the spatial scale of the RSEI spatial discretization degree. It can more comprehensively explain the relationship between explanatory variables and dependent variables, and to a certain extent can provide decision support and basis for planning and design. The identification of geographic attributes can support more accurate and effective RSEI spatial control and protection modes and the exploration of the RSEI spatial heterogeneity. Through the factor detector, we found that the soil type had the greatest impact on the RSEI, followed by the annual average temperature, slope, annual average precipitation, and roads. The results show that suitable soil types can improve the growth of vegetation [64] and control the local climate environment in Guangzhou. A series of urban constructions have changed the soil properties of the land to a certain extent. It will affect the growth of vegetation and indirectly affect the level of the RSEI. By analyzing the analysis of the detector, we find that the significance of different variables to the RSEI will vary with the change of the interval. Among them, the effects of different sections on the RSEI were not consistent. For example, interaction explains the effect of two variables on the RSEI under the condition that one variable affects the RSEI. This provides a reference basis for us to make smart decisions to resolve the impact of synergistic effects on the RSEI under multifactor conditions.

5. Conclusions

In this article, the PCA method is used to comprehensively analyze the RSEI of Guangzhou from 2001 to 2020, and the OPGD model is used to explore the influencing factors of the RSEI. The main conclusions are as follows.

(1) From 2001 to 2020, the quality of the ecological environment in Guangzhou has significantly improved. The area of the excellent level of ecological environment quality has expanded from 1778.8311 km^2 in 2001 to 1978.9389 km^2 in 2020. The area with a bad level of ecological environment quality has dropped from 719.2413 km^2 in 2001 to 660.4146 km^2 in 2020.

(2) Based on the analysis of the R package "Relaimpo", we find that NDVI and WET contributed more to ESRI in Guangzhou, while NDBSI and LST contributed relatively less to ESRI. The results of the relative importance analysis show that WET's contribution to Guangzhou's RSEI has increased from 2001 to 2020. During this period, the Betasq model showed that the contribution rate of WET decreased by 3.07%, and the LMG, Genizi, and

CAR models all indicated that the contribution rate of WET increased by more than 20% in 2020.

(3) The results of the OPGD model show that soil type have the greatest influence on the RSEI in single factor analysis, and the Q value is 0.1360. The factor with the least influence on the RSEI is the road, and the Q value is 0.0155. The influence degree and significance of the five factors on the RSEI in different intervals are different. The annual average precipitation has the greatest impact on the RSEI when it is 146~147 mm, and when it breaks through this range, its influence begins to gradually decline. The interaction detector shows that the interaction force of the two variables, annual mean temperature, and soil type, have the strongest effect on the RSEI, with a Q value of 0.1903. The least interaction on the RSEI are the two factors of road and annual average precipitation, and the Q value is 0.0828.

Based on the remote sensing data in Guangzhou from 2001 to 2020, this paper used the principal component analysis method to establish a remote sensing ecological index coupled with the main information of four ecological indicators to evaluate the environmental quality. The OPGD model is used to analyze and discuss the influencing factors of the RSEI and their interactions. This research may provide some reference for future urban environmental monitoring, management, and sustainable governance, but the article still has some deficiencies. For example, this paper resampled the annual precipitation and temperature data in order to keep the data resolution as consistent as possible. However, this will inevitably lead to some biases between the research results and the actual situation. In addition, the impact of economic development, cultural and technological construction, and tourism planning on the environment was not included in the RSEI evaluation. In the indicators, the research results may have some deviations from the actual situation. Therefore, the above deficiencies can be further considered to further improve the accuracy and comprehensiveness of ecological environment quality in future research.

Author Contributions: M.Z., Conceptualization, Methodology, Formal analysis, Writing—original draft, and Writing—review and editing; J.L., Methodology and Writing—review and editing; S.T., Supervision; B.R., Writing—review and editing; Y.Z., Writing—review and editing; A.-A.K., Methodology and Writing—review and editing. All authors have read and agreed to the published version of the manuscript.

Institutional Review Board Statement: Not applicable.

Informed Consent Statement: Not applicable.

Data Availability Statement: Not applicable.

Conflicts of Interest: The authors declare no conflict of interest.

Appendix A

Appendix A.1

Table A1. Results of the "Relaimpo" package of the R software.

Year	Item	LMG	Betasq	Genizi	CAR
2001	WET	0.3254	0.2161	0.3104	0.3276
	NDVI	0.4935	0.5615	0.5008	0.5057
	NDBSI	0.0217	0.0260	0.0184	0.0007
	LST	0.1594	0.1965	0.1703	0.1660
2020	WET	0.4936	0.2180	0.4859	0.4953
	NDVI	0.4299	0.5785	0.4373	0.4546
	NDBSI	0.0007	0.0007	0.0008	0.0007
	LST	0.0757	0.2028	0.0761	0.0494

Table A2. Land type.

NO.	Name
18	Lakes and freshwater
27	Tide soil
38	Brown lime
40	Yellow soil
44	Rice soil
50	Yellow–red Soil
62	Riverine sand
65	Mizuna rice
68	Red soil
72	Grey tide soil
78	Crimson soil
80	Submerged rice
84	Urban area
85	River
90	Rice rinsing
102	Saline rice
107	Coastal wind and sand

References

1. Hanna, N.; Sun, P.; Sun, Q.; Li, X.; Yang, X.; Ji, X.; Zou, H.; Ottoson, J.; Nilsson, L.E.; Berglund, B.; et al. Presence of Antibiotic Residues in Various Environmental Compartments of Shandong Province in Eastern China: Its Potential for Resistance Development and Ecological and Human Risk. *Environ. Int.* **2018**, *114*, 131–142. [CrossRef] [PubMed]
2. Folke, C.; Biggs, R.; Norström, A.V.; Reyers, B.; Rockström, J. Social-Ecological Resilience and Biosphere-Based Sustainability Science. *Ecol. Soc.* **2016**, *21*, 41. [CrossRef]
3. Olander, L.P.; Johnston, R.J.; Tallis, H.; Kagan, J.; Maguire, L.A.; Polasky, S.; Urban, D.; Boyd, J.; Wainger, L.; Palmer, M. Benefit Relevant Indicators: Ecosystem Services Measures That Link Ecological and Social Outcomes. *Ecol. Indic.* **2018**, *85*, 1262–1272. [CrossRef]
4. Soulsbury, C.D.; White, P.C.L. Human–Wildlife Interactions in Urban Areas: A Review of Conflicts, Benefits and Opportunities. *Wildl. Res.* **2015**, *42*, 541. [CrossRef]
5. Zhang, M.; Zhang, C.; Kafy, A.-A.; Tan, S. Simulating the Relationship between Land Use/Cover Change and Urban Thermal Environment Using Machine Learning Algorithms in Wuhan City, China. *Land* **2022**, *11*, 14. [CrossRef]
6. Lin, Z.; Wu, C.; Hong, W. Visualization Analysis of Ecological Assets/Values Research by Knowledge Mapping. *Acta Ecol. Sin.* **2015**, *35*, 142–154. [CrossRef]
7. Raseduzzaman, M.D.; Jensen, E.S. Does Intercropping Enhance Yield Stability in Arable Crop Production? *A Meta-Analysis. Eur. J. Agron.* **2017**, *91*, 25–33. [CrossRef]
8. Sun, Z.; Sun, W.; Tong, C.; Zeng, C.; Yu, X.; Mou, X. China's Coastal Wetlands: Conservation History, Implementation Efforts, Existing Issues and Strategies for Future Improvement. *Environ. Int.* **2015**, *79*, 25–41. [CrossRef]
9. Guan, X.; Wei, H.; Lu, S.; Dai, Q.; Su, H. Assessment on the Urbanization Strategy in China: Achievements, Challenges and Reflections. *Habitat Int.* **2018**, *71*, 97–109. [CrossRef]
10. Peng, J.; Pan, Y.; Liu, Y.; Zhao, H.; Wang, Y. Linking Ecological Degradation Risk to Identify Ecological Security Patterns in a Rapidly Urbanizing Landscape. *Habitat Int.* **2018**, *71*, 110–124. [CrossRef]
11. Wang, C.; Yu, C.; Chen, T.; Feng, Z.; Hu, Y.; Wu, K. Can the Establishment of Ecological Security Patterns Improve Ecological Protection? An Example of Nanchang, China. *Sci. Total Environ.* **2020**, *740*, 140051. [CrossRef] [PubMed]
12. Zhang, M.; Chen, W.; Cai, K.; Gao, X.; Zhang, X.; Liu, J.; Wang, Z.; Li, D. Analysis of the Spatial Distribution Characteristics of Urban Resilience and Its Influencing Factors: A Case Study of 56 Cities in China. *Int. J. Environ. Res. Public Health* **2019**, *16*, 4442. [CrossRef] [PubMed]
13. Vörösmarty, C.J.; Rodríguez Osuna, V.; Cak, A.D.; Bhaduri, A.; Bunn, S.E.; Corsi, F.; Gastelumendi, J.; Green, P.; Harrison, I.; Lawford, R.; et al. Ecosystem-Based Water Security and the Sustainable Development Goals (SDGs). *Ecohydrol. Hydrobiol.* **2018**, *18*, 317–333. [CrossRef]
14. Chu, X.; Deng, X.; Jin, G.; Wang, Z.; Li, Z. Ecological Security Assessment Based on Ecological Footprint Approach in Beijing-Tianjin-Hebei Region, China. *Phys. Chem. Earth Parts ABC* **2017**, *101*, 43–51. [CrossRef]
15. Bai, Y.; Jiang, B.; Wang, M.; Li, H.; Alatalo, J.M.; Huang, S. New Ecological Redline Policy (ERP) to Secure Ecosystem Services in China. *Land Use Policy* **2016**, *55*, 348–351. [CrossRef]
16. Asif, M. Growth and Sustainability Trends in the Buildings Sector in the GCC Region with Particular Reference to the KSA and UAE. Renew. *Sustain. Energy Rev.* **2016**, *55*, 1267–1273. [CrossRef]

17. Xu, D.; Yang, F.; Yu, L.; Zhou, Y.; Li, H.; Ma, J.; Huang, J.; Wei, J.; Xu, Y.; Zhang, C.; et al. Quantization of the Coupling Mechanism between Eco-Environmental Quality and Urbanization from Multisource Remote Sensing Data. *J. Clean. Prod.* **2021**, *321*, 128948. [CrossRef]

18. Yue, H.; Liu, Y.; Li, Y.; Lu, Y. Eco-Environmental Quality Assessment in China's 35 Major Cities Based on Remote Sensing Ecological Index. *IEEE Access* **2019**, *7*, 51295–51311. [CrossRef]

19. Chen, D.; Lu, X.; Hu, W.; Zhang, C.; Lin, Y. How Urban Sprawl Influences Eco-Environmental Quality: Empirical Research in China by Using the Spatial Durbin Model. *Ecol. Indic.* **2021**, *131*, 108113. [CrossRef]

20. Sun, R.; Wu, Z.; Chen, B.; Yang, C.; Qi, D.; Lan, G.; Fraedrich, K. Effects of Land-Use Change on Eco-Environmental Quality in Hainan Island, China. *Ecol. Indic.* **2020**, *109*, 105777. [CrossRef]

21. Cao, H.; Qi, Y.; Chen, J.; Shao, S.; Lin, S. Incentive and Coordination: Ecological Fiscal Transfers' Effects on Eco-Environmental Quality. *Environ. Impact Assess. Rev.* **2021**, *87*, 106518. [CrossRef]

22. Boori, M.S.; Choudhary, K.; Paringer, R.; Kupriyanov, A. Eco-Environmental Quality Assessment Based on Pressure-State-Response Framework by Remote Sensing and GIS. Remote Sens. *Appl. Soc. Environ.* **2021**, *23*, 100530. [CrossRef]

23. Wu, X.; Zhang, H. Evaluation of Ecological Environmental Quality and Factor Explanatory Power Analysis in Western Chongqing, China. *Ecol. Indic.* **2021**, *132*, 108311. [CrossRef]

24. Lai, J.; Zou, Y.; Zhang, J.; Peres-Neto, P.R. Generalizing Hierarchical and Variation Partitioning in Multiple Regression and Canonical Analyses Using the Rdacca. Hp R Package. *Methods Ecol. Evol.* **2022**, *13*, 782–788. [CrossRef]

25. Song, Y.; Wang, J.; Ge, Y.; Xu, C. An Optimal Parameters-Based Geographical Detector Model Enhances Geographic Characteristics of Explanatory Variables for Spatial Heterogeneity Analysis: Cases with Different Types of Spatial Data. *GIScience Remote Sens.* **2020**, *57*, 593–610. [CrossRef]

26. Yan, Y.; Zhuang, Q.; Zan, C.; Ren, J.; Yang, L.; Wen, Y.; Zeng, S.; Zhang, Q.; Kong, L. Using the Google Earth Engine to Rapidly Monitor Impacts of Geohazards on Ecological Quality in Highly Susceptible Areas. *Ecol. Indic.* **2021**, *132*, 108258. [CrossRef]

27. Roy, D.P.; Kovalskyy, V.; Zhang, H.K.; Vermote, E.F.; Yan, L.; Kumar, S.S.; Egorov, A. Characterization of Landsat-7 to Landsat-8 Reflective Wavelength and Normalized Difference Vegetation Index Continuity. *Remote Sens. Environ.* **2016**, *185*, 57–70. [CrossRef]

28. Zhao, W.; Yan, T.; Ding, X.; Peng, S.; Chen, H.; Fu, Y.; Zhou, Z. Response of Ecological Quality to the Evolution of Land Use Structure in Taiyuan during 2003 to 2018. *Alex. Eng. J.* **2021**, *60*, 1777–1785. [CrossRef]

29. Li, H.; Zhang, A.; Zhao, Y.; Li, J. Remote Sensing Evaluation of Environmental Quality—A Case Study of Cixian County in Handan City. In Proceedings of the International Conference on Geo-Informatics in Sustainable Ecosystem and Society, Guangzhou, China, 21–25 November 2019; Xie, Y., Zhang, A., Liu, H., Feng, L., Eds.; Communications in Computer and Information Science. Springer: Singapore, 2019; Volume 980, pp. 463–474, ISBN 9789811370243.

30. Guha, S.; Govil, H. Annual Assessment on the Relationship between Land Surface Temperature and Six Remote Sensing Indices Using Landsat Data from 1988 to 2019. *Geocarto Int.* **2021**, 1–20. [CrossRef]

31. Roy, B.; Bari, E.; Nipa, N.J.; Ani, S.A. Comparison of Temporal Changes in Urban Settlements and Land Surface Temperature in Rangpur and Gazipur Sadar, Bangladesh after the Establishment of City Corporation. Remote Sens. *Appl. Soc. Environ.* **2021**, *23*, 100587. [CrossRef]

32. Xiong, Y.; Xu, W.; Lu, N.; Huang, S.; Wu, C.; Wang, L.; Dai, F.; Kou, W. Assessment of Spatial–Temporal Changes of Ecological Environment Quality Based on RSEI and GEE: A Case Study in Erhai Lake Basin, Yunnan Province, China. *Ecol. Indic.* **2021**, *125*, 107518. [CrossRef]

33. Li, Y.; Wu, L.; Han, Q.; Wang, X.; Zou, T.; Fan, C. Estimation of Remote Sensing Based Ecological Index along the Grand Canal Based on PCA-AHP-TOPSIS Methodology. *Ecol. Indic.* **2021**, *122*, 107214. [CrossRef]

34. Boori, M.S.; Choudhary, K.; Paringer, R.; Kupriyanov, A. Spatiotemporal Ecological Vulnerability Analysis withStatistical Correlation Based on Satellite Remote Sensing in Samara, Russia. *J. Environ. Manag.* **2021**, *285*, 112138. [CrossRef] [PubMed]

35. Ning, L.; Jiayao, W.; Fen, Q. The Improvement of Ecological Environment Index Model RSEI. *Arab. J. Geosci.* **2020**, *13*, 403. [CrossRef]

36. Liu, H.; Jiang, Y.; Misa, R.; Gao, J.; Xia, M.; Preusse, A.; Sroka, A.; Jiang, Y. Ecological Environment Changes of Mining Areas around Nansi Lake with Remote Sensing Monitoring. *Environ. Sci. Pollut. Res.* **2021**, *28*, 44152–44164. [CrossRef]

37. Dang, Y.; He, H.; Zhao, D.; Sunde, M.; Du, H. Quantifying the Relative Importance of Climate Change and Human Activities on Selected Wetland Ecosystems in China. *Sustainability* **2020**, *12*, 912. [CrossRef]

38. Santé, I.; García, A.M.; Miranda, D.; Crecente, R. Cellular Automata Models for the Simulation of Real-World Urban Processes: A Review and Analysis. *Landsc. Urban Plan.* **2010**, *96*, 108–122. [CrossRef]

39. Zhang, M.; Tan, S.; Zhang, Y.; He, J.; Ni, Q. Does land transfer promote the development of new-type urbaniza-tion? New evidence from urban agglomerations in the middle reaches of the Yangtze River. *Ecol. Indic.* **2022**, *136*, 108705. [CrossRef]

40. El Aissaoui, O.; El Alami El Madani, Y.; Oughdir, L.; Dakkak, A.; El Allioui, Y. A Multiple Linear Regression-Based Approach to Predict Student Performance. In *Advanced Intelligent Systems for Sustainable Development (AI2SD'2019)*; Ezziyyani, M., Ed.; Advances in Intelligent Systems and Computing; Springer International Publishing: Cham, Switzerland, 2020; Volume 1102, pp. 9–23, ISBN 978-3-030-36652-0.

41. Wu, J.; Kobayashi, H.; Stark, S.C.; Meng, R.; Guan, K.; Tran, N.N.; Gao, S.; Yang, W.; Restrepo-Coupe, N.; Miura, T.; et al. Biological Processes Dominate Seasonality of Remotely Sensed Canopy Greenness in an Amazon Evergreen Forest. *New Phytol.* **2018**, *217*, 1507–1520. [CrossRef]

42. Grömping, U. Variable Importance in Regression Models. Wiley Interdiscip. *Rev. Comput. Stat.* **2015**, *7*, 137–152. [CrossRef]

43. Tian, W.; Liu, Y.; Heo, Y.; Yan, D.; Li, Z.; An, J.; Yang, S. Relative Importance of Factors Influencing Building Energy in Urban Environment. *Energy* **2016**, *111*, 237–250. [CrossRef]

44. Luo, Y.; Sun, W.; Yang, K.; Zhao, L. China Urbanization Process Induced Vegetation Degradation and Improvement in Recent 20 Years. *Cities* **2021**, *114*, 103207. [CrossRef]

45. Tan, S.; Zhang, M.; Wang, A.; Ni, Q. Spatio-Temporal Evolution and Driving Factors of Rural Settlements in Low Hilly Region—A Case Study of 17 Cities in Hubei Province, China. *Int. J. Environ. Res. Public Health* **2021**, *18*, 2387. [CrossRef] [PubMed]

46. Zhao, R.; Zhan, L.; Yao, M.; Yang, L. A Geographically Weighted Regression Model Augmented by Geodetector Analysis and Principal Component Analysis for the Spatial Distribution of PM2.5. Sustain. *Cities Soc.* **2020**, *56*, 102106. [CrossRef]

47. Liu, Y.; Zhang, W.; Zhang, Z.; Xu, Q.; Li, W. Risk Factor Detection and Landslide Susceptibility Mapping Using Geo-Detector and Random Forest Models: The 2018 Hokkaido Eastern Iburi Earthquake. *Remote Sens.* **2021**, *13*, 1157. [CrossRef]

48. Wang, W.; Samat, A.; Abuduwaili, J.; Ge, Y. Quantifying the Influences of Land Surface Parameters on LST Variations Based on GeoDetector Model in Syr Darya Basin, Central Asia. *J. Arid Environ.* **2021**, *186*, 104415. [CrossRef]

49. Gu, J.; Liang, L.; Song, H.; Kong, Y.; Ma, R.; Hou, Y.; Zhao, J.; Liu, J.; He, N.; Zhang, Y. A Method for Hand-Foot-Mouth Disease Prediction Using GeoDetector and LSTM Model in Guangxi, China. *Sci. Rep.* **2019**, *9*, 17928. [CrossRef]

50. Sun, D.; Shi, S.; Wen, H.; Xu, J.; Zhou, X.; Wu, J. A Hybrid Optimization Method of Factor Screening Predicated on GeoDetector and Random Forest for Landslide Susceptibility Mapping. *Geomorphology* **2021**, *379*, 107623. [CrossRef]

51. Cook, D.F.; Ragsdale, C.T.; Major, R.L. Combining a Neural Network with a Genetic Algorithm for Process Parameter Optimization. *Eng. Appl. Artif. Intell.* **2000**, *13*, 391–396. [CrossRef]

52. Brest, J.; Maucec, M.S.; Boskovic, B. Single Objective Real-Parameter Optimization: Algorithm JSO. In Proceedings of the 2017 IEEE Congress on Evolutionary Computation (CEC), San Sebastián, Spain, 5–8 June 2017; pp. 1311–1318.

53. Jayaraman, P.; Whittle, J.; Elkhodary, A.M.; Gomaa, H. Model Composition in Product Lines and Feature Interaction Detection Using Critical Pair Analysis. In *Model Driven Engineering Languages and Systems*; Engels, G., Opdyke, B., Schmidt, D.C., Weil, F., Eds.; Lecture Notes in Computer Science; Springer Berlin Heidelberg: Berlin/Heidelberg, Germany, 2007; Volume 4735, pp. 151–165, ISBN 978-3-540-75208-0.

54. Siegmund, N.; Kolesnikov, S.S.; Kastner, C.; Apel, S.; Batory, D.; Rosenmuller, M.; Saake, G. Predicting Performance via Automated Feature-Interaction Detection. In Proceedings of the 2012 34th International Conference on Software Engineering (ICSE), Zurich, Switzerland, 2–9 June 2012; pp. 167–177.

55. Zhao, Y.; Liu, L.; Kang, S.; Ao, Y.; Han, L.; Ma, C. Quantitative Analysis of Factors Influencing Spatial Distribution of Soil Erosion Based on Geo-Detector Model under Diverse Geomorphological Types. *Land* **2021**, *10*, 604. [CrossRef]

56. Shi, T.; Hu, Z.; Shi, Z.; Guo, L.; Chen, Y.; Li, Q.; Wu, G. Geo-Detection of Factors Controlling Spatial Patterns of Heavy Metals in Urban Topsoil Using Multi-Source Data. *Sci. Total Environ.* **2018**, *643*, 451–459. [CrossRef] [PubMed]

57. Zhu, L.; Meng, J.; Zhu, L. Applying Geodetector to Disentangle the Contributions of Natural and Anthropogenic Factors to NDVI Variations in the Middle Reaches of the Heihe River Basin. *Ecol. Indic.* **2020**, *117*, 106545. [CrossRef]

58. Zha, X.; Gao, X. Ecological Analysis of Kashin-Beck Osteoarthropathy Risk Factors in Tibet's Qamdo City, China. *Sci. Rep.* **2019**, *9*, 2471. [CrossRef]

59. Xu, H.; Wang, M.; Shi, T.; Guan, H.; Fang, C.; Lin, Z. Prediction of Ecological Effects of Potential Population and Impervious Surface Increases Using a Remote Sensing Based Ecological Index (RSEI). *Ecol. Indic.* **2018**, *93*, 730–740. [CrossRef]

60. Shan, W.; Jin, X.; Ren, J.; Wang, Y.; Xu, Z.; Fan, Y.; Gu, Z.; Hong, C.; Lin, J.; Zhou, Y. Ecological Environment Quality Assessment Based on Remote Sensing Data for Land Consolidation. *J. Clean. Prod.* **2019**, *239*, 118126. [CrossRef]

61. Yuan, B.; Fu, L.; Zou, Y.; Zhang, S.; Chen, X.; Li, F.; Deng, Z.; Xie, Y. Spatiotemporal Change Detection of Ecological Quality and the Associated Affecting Factors in Dongting Lake Basin, Based on RSEI. *J. Clean. Prod.* **2021**, *302*, 126995. [CrossRef]

62. Chen, W.Y. Environmental Externalities of Urban River Pollution and Restoration: A Hedonic Analysis in Guangzhou (China). *Landsc. Urban Plan.* **2017**, *157*, 170–179. [CrossRef]

63. Xie, L.; Xia, B.; Hu, Y.; Shan, M.; Le, Y.; Chan, A.P.C. Public Participation Performance in Public Construction Projects of South China: A Case Study of the Guangzhou Games Venues Construction. *Int. J. Proj. Manag.* **2017**, *35*, 1391–1401. [CrossRef]

64. Yibo, Y.; Ziyuan, C.; Xiaodong, Y.; Simayi, Z.; Shengtian, Y. The Temporal and Spatial Changes of the Ecological Environment Quality of the Urban Agglomeration on the Northern Slope of Tianshan Mountain and the Influencing Factors. *Ecol. Indic.* **2021**, *133*, 108380. [CrossRef]